



**HAL**  
open science

## The *Coxiella burnetii* secreted protein kinase CstK influences vacuole development and interacts with the GTPase-activating protein TBC1D5

Eric Martinez, Sylvaine Huc-Brandt, Solène Brelle, Julie Allombert, Franck Cantet, Laila Gannoun-Zaki, Mélanie Burette, Marianne Martin, François Letourneur, Matteo Bonazzi, et al.

### ► To cite this version:

Eric Martinez, Sylvaine Huc-Brandt, Solène Brelle, Julie Allombert, Franck Cantet, et al.. The *Coxiella burnetii* secreted protein kinase CstK influences vacuole development and interacts with the GTPase-activating protein TBC1D5. *Journal of Biological Chemistry*, 2020, 295 (21), pp.7391-7403. 10.1074/jbc.RA119.010112 . hal-02322148v2

**HAL Id: hal-02322148**

**<https://hal.umontpellier.fr/hal-02322148v2>**

Submitted on 17 Nov 2020

**HAL** is a multi-disciplinary open access archive for the deposit and dissemination of scientific research documents, whether they are published or not. The documents may come from teaching and research institutions in France or abroad, or from public or private research centers.

L'archive ouverte pluridisciplinaire **HAL**, est destinée au dépôt et à la diffusion de documents scientifiques de niveau recherche, publiés ou non, émanant des établissements d'enseignement et de recherche français ou étrangers, des laboratoires publics ou privés.

# The secreted protein kinase CstK from *Coxiella burnetii* influences vacuole development and interacts with the GTPase-activating host protein TBC1D5

Eric Martinez<sup>1,#</sup>, Sylvaine Huc-Brandt<sup>2,#</sup>, Solène Brelle<sup>2</sup>, Julie Allombert<sup>1</sup>, Franck Cantet<sup>1</sup>, Laila Gannoun-Zaki<sup>2</sup>, Mélanie Burette<sup>1</sup>, Marianne Martin<sup>2</sup>, François Letourneur<sup>2</sup>, Matteo Bonazzi<sup>1,\*</sup> and Virginie Molle<sup>2,\*</sup>

<sup>1</sup>IRIM, CNRS, Université de Montpellier, Montpellier, France

<sup>2</sup>Laboratory of Pathogen Host Interactions, Université de Montpellier, CNRS, UMR 5235, Montpellier, France

Running title: *CstK affects C. burnetii vacuole biogenesis*

## \*Corresponding author:

VM: Tel: (+33) 4 67 14 47 25, E-mail: virginie.molle@umontpellier.fr

MB: Tel: (+33) 4 34 35 94 59, E-mail: matteo.bonazzi@irim.cnrs.fr

# Both authors contributed equally to this manuscript

**Keywords:** *Coxiella burnetii*, secreted kinase, phosphorylation, serine/threonine/tyrosine protein kinase, parasitophorous vacuole, host substrates, Q fever, bacterial effector, virulence factor

The authors declare that they have no conflicts of interest with the contents of this article.

## ABSTRACT

The intracellular bacterial pathogen *Coxiella burnetii* is the etiological agent of the emerging zoonosis Q fever. Crucial to its pathogenesis is type 4b secretion system (T4SS)-mediated secretion of bacterial effectors into host cells that subvert host cell membrane trafficking, leading to the biogenesis of a parasitophorous vacuole for intracellular replication. The characterization of prokaryotic Serine/Threonine Protein Kinases (STPKs) in bacterial pathogens is emerging as an important strategy to better understand host-pathogen interactions. In this study, we investigated CstK (for *Coxiella* ser/thr Kinase), a protein kinase identified in *C. burnetii* by *in silico* analysis. We demonstrate that this putative protein kinase undergoes autophosphorylation on Thr and Tyr residues, and phosphorylates a classical eukaryotic protein kinase substrate *in vitro*. This dual Thr-Tyr kinase activity is also observed for a eukaryotic dual-specificity Tyr phosphorylation-regulated kinase class. We found that CstK is translocated during infections and localizes to *Coxiella*-containing vacuoles (CCVs). Moreover, a CstK-overexpressing *C. burnetii* strain displayed a severe CCV development phenotype, suggesting that CstK fine-tunes CCV biogenesis during the infection. Protein-protein interaction experiments identified the Rab7 GTPase-activating protein (GAP) TBC1D5 as a candidate CstK-specific

target, suggesting a role for this host GAP in *Coxiella* infections. Indeed, CstK colocalized with TBC1D5 in non-infected cells, and TBC1D5 was recruited to CCVs in infected cells. Accordingly, TBC1D5 depletion from infected cells significantly affected CCV development. Our results indicate that CstK functions as a bacterial effector protein that interacts with the host protein TBC1D5 during vacuole biogenesis and intracellular replication.

Signal transduction is an essential and universal function that allows all cells, from prokaryotes to eukaryotes, to translate environmental signals to adaptive changes. By this mechanism, extracellular inputs propagate through complex signaling networks whose activity is often regulated by reversible protein phosphorylation. Signaling mediated by Serine/Threonine/Tyrosine protein phosphorylation has been extensively studied in eukaryotes, however, its relevance in prokaryotes has only begun to be appreciated. The recent discovery that bacteria also use Ser/Thr/Tyr kinase-based signaling pathways has opened new perspectives to study environmental adaptation, especially in the case of bacterial pathogens, with respect to host infection (1). Thus, advances in genetic strategies and genome sequencing have revealed the existence of "eukaryotic-like" serine/threonine protein kinases (STPKs) and phosphatases in a number of prokaryotic organisms

(2), including pathogens such as, *Streptococcus* spp. (3-6), *Mycobacteria* (7-12), *Yersinia* spp. (13,14), *Listeria monocytogenes* (15,16), *Pseudomonas aeruginosa* (17), *Enterococcus faecalis* (18) or *Staphylococcus aureus* (19,20). Consequently, the study of STPKs in human bacterial pathogens is emerging as an important strategy to better understand host-pathogen interactions and develop new, targeted antimicrobial therapies. However, if on one hand it is clear that STPKs and phosphatases regulate important functions in bacterial pathogens, their signal transduction mechanism remains ill-defined and restricted to a limited number of microbes.

Importantly, STPKs expressed by pathogenic bacteria can either act as key regulators of important microbial processes, or be translocated by secretion systems to interact with host substrates, thereby subverting essential host functions including the immune response, cell shape and integrity (21). Phosphorylation of host substrates has been demonstrated for some bacterial STPKs, whereas others seem to require their kinase activity but their phosphorylated substrates remain to be identified (21). Therefore, biochemical mechanisms of these pathogen-directed targeted perturbations in the host cell-signaling network are being actively investigated and STPKs are proving to be molecular switches that play key roles in host-pathogen interactions (21).

Among emerging human pathogens, *Coxiella burnetii* is a highly infectious bacterium, responsible for the zoonosis Q fever, a debilitating flu-like disease leading to large outbreaks with a severe health and economic burden (22-24). The efficiency of infections by *C. burnetii* is likely associated with the remarkable capacity of this bacterium to adapt to environmental as well as intracellular stress. Indeed, outside the host, *C. burnetii* generates pseudo-spores that facilitate its airborne dissemination. *C. burnetii* has developed a unique adaptation to the host, being the only bacterium that thrives in an acidic compartment containing active lysosomal enzymes. Upon host cell invasion, bacteria reside within membrane-bound compartments that passively traffic through the endocytic maturation pathway, progressively acquiring early and late endocytic markers such as Rab5 and Rab7, respectively (25). Fusion of *Coxiella*-containing vacuoles (CCVs) with late endosomes and lysosomes is accompanied by the acidification of the endosomal environment, which is required to activate the translocation of bacterial effector proteins by a Dot/Icm Type 4b Secretion System (T4SS) (26). Some of these effectors modulate

important signaling pathways of infected cells, including apoptosis and inflammasome activation (27-29), whereas others are essential for the development of the intracellular replicative niche. Among these CvpB and CvpF have been recently implicated in the manipulation of autophagy for optimal vacuole development (30-33). *C. burnetii* genome analysis revealed a close homology to the facultative intracellular pathogen *Legionella pneumophila*, in particular at the level of Dot/Icm core genes (34). *In silico* analysis identified over 100 candidate effector proteins encoded in the *C. burnetii* genome, some of which have been validated for secretion using either *C. burnetii* or *L. pneumophila* as a surrogate model (26,35,36). In this study, we investigated the candidate effector CBU\_0175, which encodes a unique putative *Coxiella* Ser/Thr kinase (CstK). We demonstrated CstK translocation by *C. burnetii* during infection and we reported its localization at CCVs. *In vitro* kinase assays revealed that CstK undergoes autophosphorylation on Thr and Tyr residues, and displays a 'bona fide' kinase activity towards a test substrate of eukaryotic protein kinases. Furthermore, the identification of the Rab7 GTP-activating protein (GAP) TBC1D5 as a CstK interactor suggests that this protein might be involved during infection to facilitate CCVs biogenesis. Indeed, TBC1D5 is actively recruited at CCVs during *Coxiella* infections and TBC1D5-targeting siRNAs significantly affect CCVs development. Our data provide the first evidence that a *C. burnetii* secreted kinase might control host cell infection.

## RESULTS

***Coxiella burnetii* genome encodes a single putative protein kinase.** *In silico* analysis of the virulent *C. burnetii* strain RSA493 NMI genome revealed only one gene encoding a putative Serine/Threonine Protein Kinase (STPK). To date, no STPKs have been characterized in this organism. This gene was named *cstK* for *C. burnetii* serine threonine Kinase and encodes a 246 amino acids protein with an estimated molecular mass of 31 kDa. The gene coding for *cstK* is flanked by genes CBU\_0174 (which encodes an hypothetical protein) and CBU\_0176, a gene coding for the serine protease domain-containing protein degP.1. Of note, these genes are not part of an operon (Fig. 1A). InterProScan analysis of CstK revealed the presence of most of the essential amino acids and sequence subdomains characterizing the Hanks family of eukaryotic-like protein kinases (37). CstK shares a common eukaryotic protein kinases

superfamily fold with two lobes and a Gly-rich loop. These include the central core of the catalytic domain, and the invariant lysine residue in the consensus motif within subdomain II, which is usually involved in the phosphate transfer reaction and required for the autophosphorylating activity of eukaryotic STPKs (Fig. 1A) (37-39). The activation loop in the catalytic domain is particularly short in CstK, and the DFG motif is substituted by a GLG motif. Interestingly, the transmembrane domain usually present in classical prokaryotic STPKs is lacking in CstK, thus it is a so-called cytoplasmic STPK.

**CstK is a Dot/Icm effector protein.** Bioinformatics analysis using the prediction software S4TE 2.0 (40) indicated that CstK harbors features corresponding to secreted effector proteins, including a promoter motif typically found in effector proteins from intra-vacuolar bacterial pathogens, suggesting that CstK is indeed a *Coxiella* effector protein (Fig. 1A). Consistently, previous studies by Chen and colleagues have shown that CstK is secreted in a T4SS-dependent manner by the surrogate host *L. pneumophila*, albeit with low efficiency (36). In order to validate CstK secretion in *C. burnetii*, we engineered plasmids encoding, either CstK or CvpB (a known *C. burnetii* effector protein) (30), fused to Beta-Lactamase (BLAM) and expressed in wt *Coxiella Tn1832* (a *C. burnetii* transposon mutant expressing GFP and that phenocopies wild-type *C. burnetii*) or the Dot/Icm-defective *dotA::Tn* mutant, also expressing GFP. By means of a BLAM secretion assay, we could observe that BLAM-CstK was secreted by wt *Coxiella* at 48 and 72 hours, but not at 24 hours post-infection (Fig. 1B). Secretion of BLAM-CvpB or BLAM-CstK was not detectable in cells infected with the *dotA::Tn* strain, indicating that both CvpB and CstK are *C. burnetii* Dot/Icm substrates (Fig. 1B). Next, the intracellular localization of CstK was investigated by ectopically expressing HA-tagged CstK either in non-infected or wt *C. burnetii*-infected U2OS cells. In non-infected cells, CstK localized at intracellular compartments that were negative for the lysosomal marker LAMP1, whereas it was recruited at CCVs (as revealed by the co-localization with LAMP1) in infected cells (Fig. 1C).

**CstK displays autokinase and protein kinase activities.** To determine whether CstK is a functional protein kinase, this protein was overproduced in *E. coli* and purified as a recombinant protein fused to glutathione *S*-transferase (GST) tag. The purified tagged CstK

protein (Fig. 2A, upper panel) was then assayed for autokinase activity in presence of the phosphate donor [ $\gamma$ -<sup>33</sup>P]ATP. As shown in Fig. 2A (lower panel), CstK incorporated radioactive phosphate from [ $\gamma$ -<sup>33</sup>P]ATP, generating a radioactive signal corresponding to the expected size of the protein isoform, strongly suggesting that this kinase undergoes autophosphorylation. To confirm CstK autophosphorylation and exclude that contaminant kinase activities from *E. coli* extracts might phosphorylate CstK, we mutated the conserved Lys55 residue present in subdomain II into CstK by site-directed mutagenesis. Indeed protein sequence analysis revealed that Lys55 in CstK is similarly positioned as a conserved Lys residue usually involved in the phosphotransfer reaction and also required for the autophosphorylating activity of eukaryotic-like STPKs (37,38). Thus, Lys55 was substituted by a Met residue, the mutated form of CstK, CstK\_K55M, was purified as described above (Fig. 2A, upper panel) and it was then tested for autophosphorylation in presence of [ $\gamma$ -<sup>33</sup>P]ATP. As expected, no radioactive signal could be detected (Fig. 2A, lower panel), thus establishing that CstK displayed autophosphorylation activity. A kinetic analysis of CstK phosphorylation was next performed to determine the initial CstK phosphorylation rate (Fig. 2B). Incorporation of  $\gamma$ -phosphate occurred rapidly, reaching about 50% of its maximum rate within 5 min of reaction. This autokinase activity was dependent on bivalent cations such as Mg<sup>2+</sup> and Mn<sup>2+</sup> in the range of 5mM, thus in correlation with concentrations required for canonical STPK activity, as shown in Fig. 2C, and abolished by addition of 20 mM EDTA chelating all the divalent cations available (data not shown).

The recombinant CstK protein was further characterized by studying its ability to phosphorylate exogenous proteins and was thus assayed for *in vitro* phosphorylation of the general eukaryotic protein kinase substrate, myelin basic protein (MBP), in the presence of [ $\gamma$ -<sup>33</sup>P]ATP. MBP is a commonly used substrate for both Ser/Thr and Tyr kinases. A radiolabeled signal at the expected 18-kDa molecular mass of MBP was detected, thus demonstrating that CstK phosphorylates protein substrates such as MBP (Fig. 2A). As expected, the CstK\_K55M mutant did not phosphorylate MBP. Altogether, these data indicate that *in vitro*, CstK possesses intrinsic autophosphorylation activity and displays kinase functions for exogenous substrates.

#### **Identification of CstK autophosphorylation sites.**

To determine the specificity of this kinase, we next identified its autophosphorylation sites. A mass

spectrometry approach was used since this technique allows precise characterization of post-translational modifications including phosphorylation (41,42). NanoLC/nanospray/tandem mass spectrometry (LC-ESI/MS/MS) was applied for the identification of phosphorylated peptides and for localization of phosphorylation sites in CstK. This approach led to 97% of sequence coverage, while the remaining residues uncovered that did not include Ser, Thr or Tyr residues.

As detailed in Table 3, analysis of tryptic digests allowed the characterization of three phosphorylation sites in CstK. Surprisingly, unlike classical Ser/Thr or Tyr kinases, CstK was phosphorylated on two Tyr residues (Y14 and Y209), in addition to one Thr site (T232). Since protein sequence analysis did not reveal a classical activation loop in this kinase, the contribution of T232, Y14 and Y209 to CstK kinase activity was individually assessed. Hence, these residues were mutated either to phenylalanine to replace tyrosine residues or alanine to replace threonine residue, generating the single mutants CstK\_Y14F, CstK\_Y209F, and CstK\_T232A as well as the CstK\_Y14F/Y209F/T232A triple mutant (CstK\_FFA). Next, *in vitro* kinase assays with [ $\gamma$ -<sup>33</sup>P]ATP were carried out and revealed that maximum loss in CstK autophosphorylation activity was observed in the CstK\_Y14F mutant (Fig. 2D), suggesting that this site is central for CstK activation. In contrast, the CstK\_Y209F mutant exhibited a slight hyperphosphorylation, which might indicate that Y209 only plays an accessory role in controlling CstK autophosphorylation (Fig. 2D). Finally, the CstK\_T232A mutant showed a reduced CstK phosphorylation and displayed diminished kinase activity towards the exogenous substrate MBP (Fig. 2D). Note that mutating all three autophosphorylation sites fully abrogated CstK kinase activity (Fig. 2D). These results indicate that Y14 and T232 are the major phosphorylation sites in CstK and strongly suggest that CstK might be a dual specificity (Thr/Tyr) kinase.

#### ***CstK activity and phosphorylated state affect its intracellular localization.***

Next, we ectopically expressed HA-tagged CstK, CstK\_K55M and CstK\_FFA derivatives in non-infected and *C. burnetii* infected U2OS cells, to investigate its intracellular localization. CstK mainly localized at vesicular compartments in non-infected cells, and accumulated at CCVs upon *C. burnetii* infection, suggesting an active role in the biogenesis of this compartment (Fig. 1C). Interestingly, the inactive CstK\_K55M mutant

localized at vesicular structures positive for the lysosomal marker LAMP1 but not at CCVs while the non-phosphorylated CstK\_FFA displayed a diffuse localization in the cytosol of transfected cells (Fig. 2E). Overall, these data suggest that the kinase activity and phosphorylated state of CstK play an important role in its localization in cells.

***CstK regulates vacuole development and C. burnetii replication within infected cells.*** As a first step towards the understanding of CstK functions in the course of infection, and to appreciate the extent to which this kinase is required for growth and viability of *C. burnetii*, we attempted to inactivate the corresponding chromosomal gene. Unfortunately, after several attempts we were unable to generate a null mutant suggesting that *cstK* might be essential. However, we had previously isolated a *C. burnetii* mutant (*Tn2496*) carrying a transposon insertion allowing GFP expression at position 156783, 32 bp upstream of the starting codon of *cstK* (43) (Fig. 1A). To determine the effect of this transposon insertion on *cstK* gene expression, we assessed the expression level of *cstK* mRNA from wt *C. burnetii* and *Tn2496* strains. Surprisingly, *cstK* expression was significantly upregulated in the mutant strain, suggesting that the transposon insertion may have released a transcriptional negative regulation (Fig. 3A). This suggested that a putative transcriptional regulator might bind the *cstK* promoter and control its activity during host invasion.

We next examined the effects of CstK overexpression on *C. burnetii* infections by challenging Vero cells either with wt *C. burnetii*, the Dot/Icm-defective *dotA::Tn* mutant or the *Tn2496* mutant. Intracellular growth of the CstK overexpressing strain was significantly reduced over 7 days of infection with an intermediate phenotype between wt and the *dotA::Tn* mutant (Fig. 3B). Accordingly, multiparametric phenotypic profile analysis of the *Tn2496* mutant indicated that this strain exhibited a major defect in CCV development as compared to wt *C. burnetii* (Fig. 3C & D). To further investigate the effects of CstK overexpression on *C. burnetii* infections, GFP-expressing *C. burnetii* were transformed with plasmids expressing HA-tagged wt CstK or its corresponding mutants (CstK\_K55M and CstK\_FFA) under the control of an IPTG promoter. U2OS cells expressing cytoplasmic mCherry were challenged with the three *C. burnetii* strains in the presence or absence of IPTG. After 6 days of infection, cells were fixed, labelled with Hoechst and anti-LAMP1 antibody to visualize host cells nuclei and CCVs respectively, and

processed for automated image analysis. In all cases, the overexpression of CstK was detrimental for CCVs biogenesis and bacterial replication (Fig. 3E). Next, U2OS cells were challenged either with wt *C. burnetii*, the GFP-expressing *Tn2496* mutant strain or a combination of the two for 6 days (Fig. 3F). Cells were then fixed and labelled with an anti-*C. burnetii* antibody to label both bacteria strains and incubated with Hoechst to visualize host cells nuclei (Fig. 3F). Automated image analysis was then used to determine the effects of CstK overexpression on the replication of wt bacteria, in trans. Co-infections resulted in a significant increase in the size of *Tn2496* colonies, indicating that wt *C. burnetii* can partially restore the growth of the CstK-overexpressing strain (Fig. 3G). However, a significant decrease in the size of bacterial colonies labelled by the anti-*C. burnetii* antibodies indicated that CstK-overexpression has a detrimental effect in trans, on the development of wt bacteria (Fig. 3G). Of note, vacuoles harboring wt or mutant colonies alone were never observed in co-infection experiments. Therefore, we concluded that CstK participates in the formation of the *C. burnetii* replicative vacuole, and that its expression must be finely tuned for optimal intracellular replication.

#### ***CstK specifically interacts with host cell proteins.***

Since CstK is a secreted protein, we assume that this kinase would interfere with host cell signal transduction pathways to subvert host cell defenses to the benefit of the bacteria. To identify host cell proteins that could interact with CstK, we made use of the model amoeba *Dictyostelium discoideum*. *D. discoideum* is a eukaryotic professional phagocyte amenable to genetic and biochemical studies. Lysate from cells overexpressing CstK tagged with a C-terminal FLAG epitope (CstK-FLAG) was incubated with beads coupled to an anti-FLAG antibody. Beads were extensively washed, and bound proteins were separated by SDS-PAGE before mass-spectrometry analysis. Among the putative interactants of CstK identified by this approach, some were discarded on the basis of their intracellular localization while other retained candidates were mostly involved in the endocytic pathway (Table S1). Among these, the Rab GAP/TBC domain-containing protein, DDB\_G0280253 (UniProtKB - Q54VM3), is a 136.4 kDa protein homologous to mammalian TBC1D5 (<http://dictybase.org>), a GTPase-activating protein (GAP) for Rab7a and Rab7b (44-46) that acts as a molecular switch between the endosomal and the autophagy pathway (47). Given the recently reported implication of TBC1D5 in the biogenesis of *L. pneumophila*-containing vacuoles

(48) and the role of autophagy in the biogenesis of CCVs (25,31,49), we aimed at validating the interaction between human TBC1D5 (Hs-TBC1D5) and CstK in HEK-293T cells. Cells co-expressing Hs-TBC1D5-GFP and HA-CstK or CstK mutants were used for immunoprecipitation using anti-HA beads. Wild-type and CstK derivatives were detected as co-immunoprecipitated in presence of Hs-TBC1D5-GFP, thus confirming that Hs-TBC1D5 is a bona fide CstK interactant (Fig. 4A). Significantly higher levels of TBC1D5 were co-immunoprecipitated by the CstK mutants suggesting that the interaction might be increased in the absence of phosphorylation turnover of the kinase (Fig 4A, lower panel). Interestingly, the interaction is not dependent on the phosphorylation status of CstK as the K55M mutant or the triple FFA mutant are still able to interact. Other candidates identified by mass spectrometry are currently being investigated.

#### ***TBC1D5 is recruited at CCVs and regulates their biogenesis.***

Given its recently reported role in the development of *L. pneumophila*-containing vacuoles, we investigated the localization of TBC1D5 in U2OS cells infected either with wt *C. burnetii*, the CstK-overexpressing strain *Tn2496* or the Dot/Icm-defective mutant *dotA::Tn*. Consistently with previous studies demonstrating a role in the activation of Rab7a and b, TBC1D5 seems to accumulate specifically at CCVs in a Dot/Icm-independent manner as the eukaryotic protein was found at CCVs generated by all *C. burnetii* (wt, the *Tn2496* and the *dotA::Tn* Fig. 4B and Supplementary Fig.1). Next, we used siRNA to deplete cells of TBC1D5 prior to *C. burnetii* infection, to investigate a possible role in CCVs development and intracellular bacterial replication. Indeed, vacuole development was significantly reduced in cells exposed to Hs-TBC1D5-targeted siRNAs as opposed to cells treated with non-targeting siRNA oligonucleotides (Fig. 4C).

#### ***TBC1D5 is not phosphorylated in vitro by recombinant CstK.***

We assessed whether CstK might phosphorylate the recombinant Hs-TBC1D5. Despite the *in silico* prediction of several Ser/Thr and Tyr phosphorylatable residues in Hs-TBC1D5, we failed to detect Hs-TBC1D5 phosphorylation using several *in vitro* kinases assays (Supplementary Fig.2). In addition, Hs-TBC1D5 phosphorylation status was also investigated upon transfection with CstK or its inactive derivative (K55M) followed by Hs-TBC1D5 immunoprecipitation. No

phosphorylation could be detected in our experimental conditions.

## DISCUSSION

Bacterial Ser/Thr/Tyr kinases expressed by pathogenic bacteria can either act as key regulators of important microbial processes, or be translocated by secretion systems to interact with host substrates, thereby our results provide the first biochemical analysis of the secreted *C. burnetii* kinase CstK and its involvement in the process of infection and CCVs development. Importantly, CstK presents important differences as compared to classical Ser/Thr kinases. In particular, we provided evidence that CstK is a dual kinase able to autophosphorylate on Thr and Tyr residues. Moreover, the observation that a transposon insertion 32 bp upstream of the *cstK* starting codon leads to an increase in the levels of *cstK* mRNAs was indicative of the presence of a negative transcriptional regulation of gene expression, suggesting a fine tuning of the levels of CstK. Indeed, the *Tn2496* mutant displays a severe CCV biogenesis defect when used to challenge U2OS cells, highlighting the importance of regulating *cstK* expression during *C. burnetii* infections. Accordingly, inducing the expression of wt CstK in wt *C. burnetii* severely impairs CCVs development and bacterial replication. Co-infection experiments demonstrated that CstK overexpression can also act in trans, by perturbing the intracellular replication of wt *C. burnetii*. The identification of candidate eukaryotic interactors of CstK further corroborated a role of the bacterial kinase in subverting host functions during infection. Here we confirmed that CstK interacts with TBC1D5, but we failed to detect phosphorylation of the eukaryotic target by CstK. Though we cannot exclude that TBC1D5 is a genuine CstK substrate *in vivo* as the lack of phosphorylation of host interactors of bacterial STPKs is not uncommon. Interaction between STPKs and host proteins might as well perturb protein interaction networks at play in host cells (21). Indeed, the induced overexpression of CstK mutants lacking kinase activity in wt *C. burnetii* impaired CCVs development to the same extent as the overexpression of wt CstK. The biochemical mechanisms of these pathogen-directed targeted perturbations of host cell-signaling networks are being actively investigated. Regardless, siRNA depletion of TBC1D5 in *C. burnetii*-infected cells points at a role of the eukaryotic protein in CCVs development. In mammals, TBC1D5 was suggested to function as a molecular switch between endosomal and autophagy pathways.

Indeed TBC1D5 associates the retromer VPS29 subunit involved in endosomal trafficking, and upon autophagy induction, the autophagy ubiquitin-like protein LC3 can displace VPS29, thus orienting TBC1D5 functions towards autophagy instead of endosomal functions (47). It is thus tempting to propose that CstK might interfere with this tight regulation between TBC1D5, LC3 and VPS29, and redirect TBC1D5 functions to support efficient *C. burnetii* intracellular replication. Further work will need to be carried out to decipher how CstK recognizes these host substrates and how they participate in the establishment of *C. burnetii* parasitophorous vacuoles. Another perspective of this work is the opening of a new field of investigation for future drug development to fight this pathogen. Because CstK seems to be essential, specific inhibitors of this kinase preventing *C. burnetii* growth would be extremely useful for the development of new therapies.

## EXPERIMENTAL PROCEDURES

**Bacterial strains and growth conditions.** Bacterial strains and plasmids are described in Table 1. Strains used for cloning and expression of recombinant proteins were *Escherichia coli* TOP10 (Invitrogen) and *E. coli* BL21 (DE3)Star (Stratagene), respectively. *E. coli* cells were grown and maintained at 25 °C in LB medium supplemented with 100 µg/ml ampicillin when required. *Coxiella burnetii* RSA439 NMII and transposon mutants *Tn1832*, *Tn2496*, and *dotA::Tn* were grown in ACCM-2 (45) supplemented with chloramphenicol (3 mg/ml) in a humidified atmosphere of 5% CO<sub>2</sub> and 2.5% O<sub>2</sub> at 37 °C.

**Cloning, expression and purification of CstK derivatives.** The *cstK* (*CBU\_0175*) gene was amplified by PCR using *Coxiella burnetii* RSA439 NMII chromosomal DNA as a template with the primers listed in Table 2 containing a *Bam*HI and *Hind*III restriction site, respectively. The corresponding amplified product was digested with *Bam*HI and *Hind*III, and ligated into the bacterial pGEX(M) plasmid, that includes a N-terminal GST-tag, thus generating pGEX(M)<sub>*cstK*</sub>. pGEX(M)<sub>*cstK*</sub> derivatives harboring different mutations were generated by using the QuikChange Site-Directed Mutagenesis Kit (Stratagene, La Jolla, CA), and resulted in the construction of plasmids detailed in Table 2. For overexpression assays, *cstK* and its derivatives were cloned in the pJA-LACO-4xHA vector (30) using *Kpn*I and *Bam*HI restriction sites. All constructs were verified by DNA sequencing.

Transformed *E. coli* BL21 Star cells with pGEX(M)<sub>cstK</sub> derivatives were grown at 16 °C in LB medium containing 1 g/liter of glucose and 100 µg/ml of ampicillin and protein synthesis induced with 0.5 mM IPTG overnight. Bacteria were disrupted by sonication (Branson, digital sonifier) and centrifuged at 14,000 rpm for 25 min. Purifications of the GST-tagged recombinants were performed as described by the manufacturer (GE Healthcare). *cstK* coding sequence was also optimized for mammalian cell expression (GenScript), amplified by PCR and cloned into pDXA-3C (50) containing a FLAG-tag for C-terminal fusion. After sequencing, the plasmid was linearized by the restriction enzyme *ScaI* and transfected in *D. discoideum* as described (51). Clone selection was made with 10 mg/ml of G418, and protein expression was assayed by Western blot analysis of *D. discoideum* crude extract with an anti-FLAG rabbit polyclonal antibody (GenScript, USA). For ectopic expression assays, *cstK*, *cstK\_K55M* and *cstK\_FFA* with optimized codons (IDT) were cloned in pRK5-HA using the primer pair CstKopt-BamHI-Fw/CstKopt-EcoRI-Rv.

**Cloning, expression and purification of TBC1D5 derivatives.** The *D. discoideum* GFP-tagged TBC1D5 was previously generated (48). Cells were grown at 22 °C in HL5 medium as previously described (51). Human TBC1D5 coding sequence was obtained from the hORFeome v8.1 (ORF 2659, Q92609, fully-sequenced cloned human ORFs in Gateway Entry clones ready for transfer to Gateway-compatible expression vectors). HsTBC1D5 coding sequence has been recombined into pEGFP-N1 RfC Destination vector by GateWay reaction (MGC Platform Montpellier) thus generating pEGFP-N1\_HsTBC1D5 coding for HsTBC1D5 with a C-terminal GFP Tag. pmCH\_Hs-TBC1D5-mCherry has been generated by the same method (MGC Platform Montpellier).

**RNA extraction and quantitative RT-PCR (qRT-PCR).** Fifty ml of *C. burnetii* culture was harvested, resuspended in 600 µL of RNA protect reagent (Qiagen) and incubated 5 min at room temperature. Bacteria were centrifuged and resuspended in 200 µl TE (10 mM Tris-HCl, 1 mM EDTA, pH 8) containing 1 mg/ml lysozyme. Bacterial suspension was incubated at room temperature for 5 min and bacteria were disrupted by vigorous vortexing for 10 sec every 2 min. 700 µl of RLT buffer from RNA easy kit (Qiagen), were added to the bacterial suspension and disruption was completed by vortexing vigorously. RNA was purified with the RNA easy kit according

to manufacturer's instructions. DNA was further removed using DNase I (Invitrogen). cDNA was produced using Superscript III reverse transcriptase (Invitrogen). Controls without reverse transcriptase were done on each RNA sample to rule out possible DNA contamination. Quantitative real-time PCR was performed using LightCycler 480 SYBR Green I Master (Roche) and a 480 light cycler instrument (Roche). PCR conditions were as follows: 3 min denaturation at 98 °C, 45 cycles of 98 °C for 5 sec, 60 °C for 10 sec and 72 °C for 10 sec. The *dotA* gene was used as internal control. The sequences of primers used for qRT-PCR are listed in Table 2. The expression level of *cstK* in the wild type strain was set at 100 and the expression levels of *cstK* in the *Tn2496* mutant were normalized to the wild type levels.

**In vitro kinase assays.** *In vitro* phosphorylation was performed with 4 µg of wild-type CstK or CstK derivatives in 20 µl of buffer P (25 mM Tris-HCl, pH 7.0; 1 mM DTT; 5 mM MnCl<sub>2</sub>; 1 mM EDTA; 50 µM ATP) with 200 µCi ml<sup>-1</sup> (65 nM) [ $\gamma$ -<sup>33</sup>P]ATP (PerkinElmer, ref: NEG 602H250UC, 3000 Ci mmol<sup>-1</sup>) for 30 min at 37 °C. For substrate phosphorylation, 4 µg of MBP (Myelin Basic Protein) (Sigma) and 4 µg of CstK were used. Each reaction mixture was stopped by addition of an equal volume of Laemmli buffer and the mixture was heated at 100 °C for 5 min. After electrophoresis, gels were soaked in 16% TCA for 10 min at 90 °C, and dried. Radioactive proteins were visualized by autoradiography using direct exposure to films.

**Mass spectrometry analysis.** For mass spectrometry analysis, CstK was phosphorylated as described above, except that [ $\gamma$ -<sup>33</sup>P]ATP was replaced with 5 mM cold ATP. Subsequent mass spectrometry analyses were performed as previously reported (52,53). Briefly, samples were submitted to trypsin digestion and analyzed using an Ultimate 3000 nano-RSLC (Thermo Scientific, San Jose California) coupled on line with a quadrupole-orbitrap Q Exactive HF mass spectrometer via a nano-electrospray ionization source (Thermo Scientific, San Jose California). Samples were injected and loaded on a C18 Acclaim PepMap100 trap-column (Thermo Scientific) and separated on a C18 Acclaim Pepmap100 nano-column (Thermo Scientific). MS data were acquired in a data dependent strategy selecting the fragmentation events based on the 20 most abundant precursor ions in the survey scan (350-1600 Th). The resolution of the survey scan was 60,000 at m/z 200 Th and for MS/MS scan the resolution was set to 15,000 at m/z 200 Th.

Peptides selected for MS/MS acquisition were then placed on an exclusion list for 30s using the dynamic exclusion mode to limit duplicate spectra. Data files were then analyzed with Proteome Discover 2.2 using the SEQUEST HT algorithm against the Uniprot *Dictyostelium discoideum* to which was included the sequence of CstK.

**C. burnetii infections.** U2OS epithelial cells were challenged either with *Coxiella burnetii* RSA439 NMII, the transposon mutants *Tn1832*, *dotA::Tn* or *Tn2496* as previously described (38,49). For co-infection experiments, cells were challenged with a 1:1 ratio of *Coxiella burnetii* RSA439 NMII and *Tn2496* transposon mutant. For gene silencing, U2OS cells were seeded at 2,000 cells per well in black, clear-bottomed, 96-well plates in triplicate and transfected with siRNA oligonucleotides 24 h later by using the RNAiMAX transfection reagent (Thermo Fisher Scientific) according to the manufacturer's recommendations. At 24 h post transfection, cells were challenged with *C. burnetii* (MOI of 100) and further incubated for 5 d. Cells were then fixed and processed for immunofluorescence. Where appropriate, anti-LAMP1 antibodies were used to label lysosomes and CCVs as previously described (54). Samples were imaged with a Zeiss Axio Imager Z1 epifluorescence microscope (Carl Zeiss, Germany) connected to a CoolSNAP HQ<sup>2</sup> CCD camera (Teledyne Photometrics, Tucson, AZ). Images were acquired with 40x oil immersion objectives and processed with Metamorph (Molecular Devices, San Jose, CA). For phenotypic screening, samples were imaged with an ArrayScan VTI Live epifluorescence automated microscope (Cellomics) equipped with an ORCA-ER CCD camera (Hamamatsu). 25 fields per well were acquired for image analysis. ImageJ and ICY software were used for image analysis and quantifications. Phenotypic profiles (expressed as z-scores) were calculated using CellProfiler, from triplicate experiments as previously described (54) following median based normalization of 96-well plates. Plates effects were corrected by the median value across wells that are annotated as control.

**Beta-lactamase translocation assay.** Effector proteins translocation assays were performed as previously described (30). Briefly, *Coxiella burnetii* *Tn1832* (wt) and *dotA::Tn* were transformed either with pXDC-Blam (negative control), pXDC-Blam-CvpB (positive control) or pXDC-Blam-CstK. Each strain was used to infect U2OS epithelial cells. After 24, 48 or 72 hours of infection, cells were loaded with the fluorescent substrate CCF4/AM (LiveBLazer-FRET B/G

loading kit; Invitrogen) in HBSS (20 mM HEPES pH 7.3) containing 15 mM probenecid (Sigma). Cells were incubated in the dark for 1 h at room temperature and imaged using an EVOS inverted fluorescence microscope. Images were acquired using DAPI and GFP filter cubes. The image analysis software CellProfiler was used to segment and identify all cells in the sample (GFP), positive cells (DAPI) and to calculate the intensity of fluorescence in each channel. The percentage of positive cells versus the total number of infected cells was then calculated and used to evaluate effector translocation.

**Immunoprecipitation from *D. discoideum* lysates.**

For immunoprecipitation assays,  $2 \times 10^7$  cells were lysed in lysis buffer (50 mM Tris-HCl pH 7.5, 300 mM NaCl, 0.5% NP40, protease inhibitors (Roche)) and cleared by centrifugation for 15 min at 14 000 rpm in a microfuge. Lysate supernatants were incubated overnight at 4 °C with anti-flag monoclonal antibody coated on agarose beads (Genscript). The beads were then washed five times in wash buffer (50 mM Tris-HCl pH 7.5, 300 mM NaCl, 0.1% NP40) and once in PBS. Bound proteins were migrated on SDS-PAGE and analyzed by LC-MS/MS.

**Cell culture, heterologous expression and anti-HA immunoprecipitation.**

HEK-293T cells were grown in DMEM (Gibco) containing 10% (vol/vol) FBS, 1% glutamax (Gibco, 200 mM stock), 0.5% Penicillin/Streptomycin (Gibco, 10000 U/mL stock) and maintained under standard conditions at 37 °C in a humidified atmosphere containing 5% CO<sub>2</sub>. Cells were transiently transfected using the jetPEI Transfection Reagent (Polyplus-Transfection Inc.) to express either Hs-TBC1D5-GFP, CstK<sub>HA</sub> derivatives, or each CstK derivatives with TBC1D5\_GFP protein. Cells were used 24h after transfection for immunoprecipitation assay. Transfected cells were washed two times in cold PBS and lysed in lysis buffer (50 mM Tris, 150 mM NaCl, 0.5 mM EDTA, 0.5 % NP40, protease and phosphatases inhibitors (Roche)). Cleared lysate (950 μL, approximately 1 mg total proteins) were incubated with anti HA magnetic Beads (Pierce) for 30 min at room temperature under gentle rotation. The beads were washed three times in lysis buffer, boiled in 2X Laemmli sample buffer and loaded on ExpressPlus™ PAGE Gels (GenScript). The eluted proteins were visualized by Western Blotting with the following antibodies: anti-HA from Chromotek, anti-GFP from Torrey Pines, donkey anti-rat or anti-rabbit from Jackson ImmunoResearch.

### **Densitometry.**

Regions of Interest (ROIs) were obtained from each band of interest and the intensity was measured using ImageLab (From Biorad). For each

band, the same ROI was used for background calculation and removal from areas adjacent to each band.

### **DATA AVAILABILITY STATEMENT**

All the data are contained in this manuscript.

### **ACKNOWLEDGMENTS**

We wish to thank the Montpellier RIO imaging facility at the University of Montpellier, member of the national infrastructure France-BioImaging, that is supported by the French National Research Agency (ANR-10-INBS-04, «Investments for the future»). We acknowledge the contribution of the Protein Science Facility of the SFR Biosciences (UMS3444/CNRS, US8/Inserm, ENS de Lyon, UCBL), especially Frédéric DELOLME and Adeline PAGE who performed the mass spectrometry analysis. This work was supported by grants from the ATIP/AVENIR Program for V.M. and M.B., the Region Occitanie for S. B., a Marie Curie CIG to E.M. (grant n. 293731), the Agence Nationale de la Recherche (ANR) Grant ANR-14-CE14-0012-01 (project AttaQ) to M.B.

### **CONFLICT OF INTEREST**

The authors declare that they have no conflicts of interest with the contents of this article.

### **REFERENCES**

1. Stancik, I. A., Sestak, M. S., Ji, B., Axelson-Fisk, M., Franjevic, D., Jers, C., Domazet-Loso, T., and Mijakovic, I. (2018) Serine/Threonine Protein Kinases from Bacteria, Archaea and Eukarya Share a Common Evolutionary Origin Deeply Rooted in the Tree of Life. *J Mol Biol* **430**, 27-32
2. Janczarek, M., Vinardell, J. M., Lipa, P., and Karas, M. (2018) Hanks-Type Serine/Threonine Protein Kinases and Phosphatases in Bacteria: Roles in Signaling and Adaptation to Various Environments. *Int J Mol Sci* **19**
3. Rajagopal, L., Clancy, A., and Rubens, C. E. (2003) A eukaryotic type serine/threonine kinase and phosphatase in *Streptococcus agalactiae* reversibly phosphorylate an inorganic pyrophosphatase and affect growth, cell segregation, and virulence. *J Biol Chem* **278**, 14429-14441
4. Hussain, H., Branny, P., and Allan, E. (2006) A eukaryotic-type serine/threonine protein kinase is required for biofilm formation, genetic competence, and acid resistance in *Streptococcus mutans*. *J Bacteriol* **188**, 1628-1632
5. Echenique, J., Kadioglu, A., Romao, S., Andrew, P. W., and Trombe, M. C. (2004) Protein serine/threonine kinase StkP positively controls virulence and competence in *Streptococcus pneumoniae*. *Infect Immun* **72**, 2434-2437
6. Jin, H., and Pancholi, V. (2006) Identification and biochemical characterization of a eukaryotic-type serine/threonine kinase and its cognate phosphatase in *Streptococcus pyogenes*: their biological functions and substrate identification. *J Mol Biol* **357**, 1351-1372
7. Av-Gay, Y., and Everett, M. (2000) The eukaryotic-like Ser/Thr protein kinases of *Mycobacterium tuberculosis*. *Trends Microbiol* **8**, 238-244
8. Chaba, R., Raje, M., and Chakraborti, P. K. (2002) Evidence that a eukaryotic-type serine/threonine protein kinase from *Mycobacterium tuberculosis* regulates morphological changes associated with cell division. *Eur J Biochem* **269**, 1078-1085
9. Wehenkel, A., Bellinzoni, M., Grana, M., Duran, R., Villarino, A., Fernandez, P., Andre-Leroux, G., England, P., Takiff, H., Cervenansky, C., Cole, S. T., and Alzari, P. M. (2008) Mycobacterial Ser/Thr protein kinases and phosphatases: physiological roles and therapeutic potential. *Biochim Biophys Acta* **1784**, 193-202
10. Molle, V., and Kremer, L. (2010) Division and cell envelope regulation by Ser/Thr phosphorylation: *Mycobacterium* shows the way. *Mol Microbiol* **75**, 1064-1077
11. Alber, T. (2009) Signaling mechanisms of the *Mycobacterium tuberculosis* receptor Ser/Thr protein kinases. *Curr Opin Struct Biol* **19**, 650-657

12. Greenstein, A. E., Grundner, C., Echols, N., Gay, L. M., Lombana, T. N., Miecskowski, C. A., Pullen, K. E., Sung, P. Y., and Alber, T. (2005) Structure/function studies of Ser/Thr and Tyr protein phosphorylation in *Mycobacterium tuberculosis*. *J Mol Microbiol Biotechnol* **9**, 167-181
13. Galyov, E. E., Hakansson, S., Forsberg, A., and Wolf-Watz, H. (1993) A secreted protein kinase of *Yersinia pseudotuberculosis* is an indispensable virulence determinant. *Nature* **361**, 730-732
14. Hakansson, S., Galyov, E. E., Rosqvist, R., and Wolf-Watz, H. (1996) The *Yersinia* YpkA Ser/Thr kinase is translocated and subsequently targeted to the inner surface of the HeLa cell plasma membrane. *Mol Microbiol* **20**, 593-603
15. Archambaud, C., Gouin, E., Pizarro-Cerda, J., Cossart, P., and Dussurget, O. (2005) Translation elongation factor EF-Tu is a target for Stp, a serine-threonine phosphatase involved in virulence of *Listeria monocytogenes*. *Mol Microbiol* **56**, 383-396
16. Lima, A., Duran, R., Schujman, G. E., Marchissio, M. J., Portela, M. M., Obal, G., Pritsch, O., de Mendoza, D., and Cervenansky, C. (2011) Serine/threonine protein kinase PrkA of the human pathogen *Listeria monocytogenes*: biochemical characterization and identification of interacting partners through proteomic approaches. *J Proteomics* **74**, 1720-1734
17. Wang, J., Li, C., Yang, H., Mushegian, A., and Jin, S. (1998) A novel serine/threonine protein kinase homologue of *Pseudomonas aeruginosa* is specifically inducible within the host infection site and is required for full virulence in neutropenic mice. *J Bacteriol* **180**, 6764-6768
18. Kristich, C. J., Wells, C. L., and Dunny, G. M. (2007) A eukaryotic-type Ser/Thr kinase in *Enterococcus faecalis* mediates antimicrobial resistance and intestinal persistence. *Proc Natl Acad Sci U S A* **104**, 3508-3513
19. Beltramini, A. M., Mukhopadhyay, C. D., and Pancholi, V. (2009) Modulation of cell wall structure and antimicrobial susceptibility by a *Staphylococcus aureus* eukaryote-like serine/threonine kinase and phosphatase. *Infect Immun* **77**, 1406-1416
20. Truong-Bolduc, Q. C., Ding, Y., and Hooper, D. C. (2008) Posttranslational modification influences the effects of MgrA on norA expression in *Staphylococcus aureus*. *J Bacteriol* **190**, 7375-7381
21. Canova, M. J., and Molle, V. (2014) Bacterial serine/threonine protein kinases in host-pathogen interactions. *J Biol Chem* **289**, 9473-9479
22. Kazar, J. (2005) *Coxiella burnetii* infection. *Ann N Y Acad Sci* **1063**, 105-114
23. Arricau-Bouvery, N., and Rodolakis, A. (2005) Is Q fever an emerging or re-emerging zoonosis? *Vet Res* **36**, 327-349
24. Madariaga, M. G., Rezai, K., Trenholme, G. M., and Weinstein, R. A. (2003) Q fever: a biological weapon in your backyard. *Lancet Infect Dis* **3**, 709-721
25. Beron, W., Gutierrez, M. G., Rabinovitch, M., and Colombo, M. I. (2002) *Coxiella burnetii* localizes in a Rab7-labeled compartment with autophagic characteristics. *Infect Immun* **70**, 5816-5821
26. Newton, H. J., McDonough, J. A., and Roy, C. R. (2013) Effector protein translocation by the *Coxiella burnetii* Dot/Icm type IV secretion system requires endocytic maturation of the pathogen-occupied vacuole. *PLoS One* **8**, e54566
27. Luhrmann, A., Nogueira, C. V., Carey, K. L., and Roy, C. R. (2010) Inhibition of pathogen-induced apoptosis by a *Coxiella burnetii* type IV effector protein. *Proc Natl Acad Sci U S A* **107**, 18997-19001
28. Klingenbeck, L., Eckart, R. A., Berens, C., and Luhrmann, A. (2013) The *Coxiella burnetii* type IV secretion system substrate CaeB inhibits intrinsic apoptosis at the mitochondrial level. *Cell Microbiol* **15**, 675-687
29. Cunha, L. D., Ribeiro, J. M., Fernandes, T. D., Massis, L. M., Khoo, C. A., Moffatt, J. H., Newton, H. J., Roy, C. R., and Zamboni, D. S. (2015) Inhibition of inflammasome activation by *Coxiella burnetii* type IV secretion system effector IcaA. *Nat Commun* **6**, 10205
30. Martinez, E., Allombert, J., Cantet, F., Lakhani, A., Yandrapalli, N., Neyret, A., Norville, I. H., Favard, C., Muriaux, D., and Bonazzi, M. (2016) *Coxiella burnetii* effector CvpB modulates phosphoinositide metabolism for optimal vacuole development. *Proc Natl Acad Sci U S A* **113**, E3260-3269
31. Siadous, F. A., Cantet, F., Van Schaik, E., Burette, M., Allombert, J., Lakhani, A., Bonaventure, B., Goujon, C., Samuel, J., Bonazzi, M., and Martinez, E. (2020) *Coxiella* effector protein CvpF subverts RAB26-dependent autophagy to promote vacuole biogenesis and virulence. *Autophagy*, 1-17

32. Newton, H. J., Kohler, L. J., McDonough, J. A., Temoche-Diaz, M., Crabill, E., Hartland, E. L., and Roy, C. R. (2014) A screen of *Coxiella burnetii* mutants reveals important roles for Dot/Icm effectors and host autophagy in vacuole biogenesis. *PLoS Pathog* **10**, e1004286
33. Latomanski, E. A., Newton, P., Khoo, C. A., and Newton, H. J. (2016) The Effector Cig57 Hijacks FCHO-Mediated Vesicular Trafficking to Facilitate Intracellular Replication of *Coxiella burnetii*. *PLoS Pathog* **12**, e1006101
34. Vogel, J. P. (2004) Turning a tiger into a house cat: using *Legionella pneumophila* to study *Coxiella burnetii*. *Trends Microbiol* **12**, 103-105
35. Carey, K. L., Newton, H. J., Luhrmann, A., and Roy, C. R. (2011) The *Coxiella burnetii* Dot/Icm system delivers a unique repertoire of type IV effectors into host cells and is required for intracellular replication. *PLoS Pathog* **7**, e1002056
36. Chen, C., Banga, S., Mertens, K., Weber, M. M., Gorbaslieva, I., Tan, Y., Luo, Z. Q., and Samuel, J. E. (2010) Large-scale identification and translocation of type IV secretion substrates by *Coxiella burnetii*. *Proc Natl Acad Sci U S A* **107**, 21755-21760
37. Hanks, S. K., and Hunter, T. (1995) Protein kinases 6. The eukaryotic protein kinase superfamily: kinase (catalytic) domain structure and classification. *Faseb J* **9**, 576-596
38. Hanks, S. K., Quinn, A. M., and Hunter, T. (1988) The protein kinase family: conserved features and deduced phylogeny of the catalytic domains. *Science* **241**, 42-52
39. Carrera, A. C., Alexandrov, K., and Roberts, T. M. (1993) The conserved lysine of the catalytic domain of protein kinases is actively involved in the phosphotransfer reaction and not required for anchoring ATP. *Proc Natl Acad Sci U S A* **90**, 442-446
40. Noroy, C., Lefrancois, T., and Meyer, D. F. (2019) Searching Algorithm for Type IV Effector proteins (S4TE) 2.0: improved tools for type IV effector prediction, analysis and comparison. *bioRxiv*
41. Fiuza, M., Canova, M. J., Zanella-Cleon, I., Becchi, M., Cozzone, A. J., Mateos, L. M., Kremer, L., Gil, J. A., and Molle, V. (2008) From the characterization of the four serine/threonine protein kinases (PknA/B/G/L) of *Corynebacterium glutamicum* toward the role of PknA and PknB in cell division. *J Biol Chem* **283**, 18099-18112
42. Molle, V., Leiba, J., Zanella-Cleon, I., Becchi, M., and Kremer, L. (2010) An improved method to unravel phosphoacceptors in Ser/Thr protein kinase-phosphorylated substrates. *Proteomics* **10**, 3910-3915
43. Martinez, E., Cantet, F., Fava, L., Norville, I., and Bonazzi, M. (2014) Identification of OmpA, a *Coxiella burnetii* protein involved in host cell invasion, by multi-phenotypic high-content screening. *PLoS Pathog* **10**, e1004013
44. Borg Distefano, M., Hofstad Haugen, L., Wang, Y., Perdreau-Dahl, H., Kjos, I., Jia, D., Morth, J. P., Neeffjes, J., Bakke, O., and Progida, C. (2018) TBC1D5 controls the GTPase cycle of Rab7b. *Journal of cell science* **131**
45. Seaman, M. N. J., Mukadam, A. S., and Breusegem, S. Y. (2018) Inhibition of TBC1D5 activates Rab7a and can enhance the function of the retromer cargo-selective complex. *Journal of cell science* **131**
46. Sun, M., Luong, G., Plastikwala, F., and Sun, Y. (2020) Control of Rab7a activity and localization through endosomal type Igamma PIP 5-kinase is required for endosome maturation and lysosome function. *FASEB J* **34**, 2730-2748
47. Popovic, D., and Dikic, I. (2014) TBC1D5 and the AP2 complex regulate ATG9 trafficking and initiation of autophagy. *EMBO reports* **15**, 392-401
48. Barlocher, K., Hutter, C. A. J., Swart, A. L., Steiner, B., Welin, A., Hohl, M., Letourneur, F., Seeger, M. A., and Hilbi, H. (2017) Structural insights into *Legionella* RidL-Vps29 retromer subunit interaction reveal displacement of the regulator TBC1D5. *Nat Commun* **8**, 1543
49. McDonough, J. A., Newton, H. J., Klum, S., Swiss, R., Agaisse, H., and Roy, C. R. (2013) Host pathways important for *Coxiella burnetii* infection revealed by genome-wide RNA interference screening. *mBio* **4**, e00606-00612
50. Manstein, D. J., Schuster, H. P., Morandini, P., and Hunt, D. M. (1995) Cloning vectors for the production of proteins in *Dictyostelium discoideum*. *Gene* **162**, 129-134
51. Alibaud, L., Cosson, P., and Benghezal, M. (2003) *Dictyostelium discoideum* transformation by oscillating electric field electroporation. *BioTechniques* **35**, 78-80, 82-73

52. Brelle, S., Baronian, G., Huc-Brandt, S., Zaki, L. G., Cohen-Gonsaud, M., Bischoff, M., and Molle, V. (2016) Phosphorylation-mediated regulation of the *Staphylococcus aureus* secreted tyrosine phosphatase PtpA. *Biochem Biophys Res Commun* **469**, 619-625
53. Baronian, G., Ginda, K., Berry, L., Cohen-Gonsaud, M., Zakrzewska-Czerwinska, J., Jakimowicz, D., and Molle, V. (2015) Phosphorylation of *Mycobacterium tuberculosis* ParB participates in regulating the ParABS chromosome segregation system. *PLoS One* **10**, e0119907
54. Martinez, E., Cantet, F., and Bonazzi, M. (2015) Generation and multi-phenotypic high-content screening of *Coxiella burnetii* transposon mutants. *Journal of visualized experiments : JoVE*, e52851
55. Beare, P. A., Sandoz, K. M., Omsland, A., Rockey, D. D., and Heinzen, R. A. (2011) Advances in genetic manipulation of obligate intracellular bacterial pathogens. *Frontiers in microbiology* **2**, 97
56. Molle, V., Kremer, L., Girard-Blanc, C., Besra, G. S., Cozzone, A. J., and Prost, J. F. (2003) An FHA phosphoprotein recognition domain mediates protein EmbR phosphorylation by PknH, a Ser/Thr protein kinase from *Mycobacterium tuberculosis*. *Biochemistry* **42**, 15300-15309
57. Charpentier, E., Anton, A. I., Barry, P., Alfonso, B., Fang, Y., and Novick, R. P. (2004) Novel cassette-based shuttle vector system for gram-positive bacteria. *Appl Environ Microbiol* **70**, 6076-6085

## FIGURE LEGENDS

**Figure 1. *CstK* is a *Dot/Icm* effector protein (A)** Schematic representation of CstK. A conserved promoter-binding domain is predicted between aa -227 and -213 (*Apm*) and the transposon insertion site for *Tn2496* is indicated. The kinase domain is predicted between aa 26 and 174 and is shown in red. The conserved lysine residue is indicated, and the phosphorylated sites are indicated by an asterisk. **(B)** BLAM secretion assay. U2OS cells were infected for 24, 48, or 72h (black, grey and white bars, respectively) with wt *C. burnetii* or the *dotA::Tn* mutant transformed with vectors expressing Beta-Lactamase alone (BLAM, negative control), BLAM-CvpB (positive control) or BLAM-CstK. Protein translocation was probed using the CCF-4 substrate. The average percentage of cells positive for cleaved CCF-4 as compared to the total number of cells was assessed. Values are mean  $\pm$  SD from 3 independent experiments. ns = non-significant; \*\*\* =  $P < 0.0001$ , one-way ANOVA, Dunnett's multiple comparison test. CstK localization. **(C)** U2OS cells ectopically expressing HA-tagged CstK (red) were either left untreated (top panels) or challenged with wt *C. burnetii* expressing GFP (green) for 3 days. Lysosomal compartments were labelled using anti-LAMP1 antibodies (blue). Scale bars 10  $\mu$ m.

**Figure 2. (A) Biochemical characterization of CstK.** Recombinant CstK derivatives were overproduced, purified on glutathione-Sepharose 4B matrix and submitted to gel electrophoresis and stained with Coomassie Blue (upper panel). *In vitro* phosphorylation assays were performed with [ $\gamma$ - $^{33}$ P]ATP for 30 min and the eukaryotic substrate myelin basic protein (MBP) when required. Proteins were analyzed by SDS-PAGE, and radioactive bands were revealed by autoradiography (lower panel). The upper bands illustrate the autokinase activity of CstK, and the lower bands represent phosphorylated MBP. Standard proteins of known molecular masses were run in parallel. **(B)** A kinetic analysis was performed by incubation of CstK with [ $\gamma$ - $^{33}$ P]ATP over different times. Proteins were analyzed by SDS-PAGE, and radioactive bands were revealed by autoradiography. **(C)** Effects of cations on autokinase activity of CstK. Purified CstK protein was subjected to *in vitro* autophosphorylation assays in the presence of 50  $\mu$ M ATP [ $\gamma$ - $^{33}$ P]ATP and 5 mM of  $Mg^{2+}$  or  $Mn^{2+}$ . Phosphoproteins were separated by SDS-PAGE and then revealed by autoradiography. **(D)** *In vitro* phosphorylation of CstK mutant derivatives. The mutated variants CstK\_Y14F (harboring a Tyr to Phe substitution at Y14), CstK\_Y209F (harboring a Tyr to Phe substitution at Y209), CstK\_T232A (harboring a Thr to Ala substitution at T232), or CstK\_Y14F/Y209F/T232A (harboring all three substitutions) were incubated in presence of [ $\gamma$ - $^{33}$ P]ATP with or without the eukaryotic substrate myelin basic protein (MBP). Samples were separated by SDS-PAGE, stained with Coomassie Blue (upper panel), and visualized by autoradiography (lower panel). The upper bands illustrate the autokinase activity of CstK, and the lower bands represent phosphorylated MBP. Standard proteins of known molecular masses were run in parallel (kDa lane). **(E)** U2OS cells ectopically expressing either HA-tagged CstK\_K55M or CstK\_FFA (red) were challenged with wt *C. burnetii* expressing GFP (green) for 3 days. Lysosomal compartments were labelled using anti-LAMP1 antibodies (blue). Scale bars 10  $\mu$ m. Inset magnification scale bars 4  $\mu$ m.

**Figure 3. CstK regulates vacuole development and *C. burnetii* replication within infected cells.** (A) Expression of *cstK* was measured by qRT-PCR from cultures of either wt *C. burnetii* or the *Tn2496* mutant strain. Values are means  $\pm$  SEM of 4 independent experiments. \*\*\*,  $p < 0.001$ , unpaired t-test. (B) Vero cells were challenged either with wt *C. burnetii*, the *dotA::Tn* mutant or the *Tn2496* mutant strains, all expressing GFP. Intracellular replication was monitored over 7 days of infection by monitoring the GFP fluorescence using a microplate reader. Values are mean  $\pm$  SD from 3 independent experiments. (C) U2OS cells were challenged either with wt *C. burnetii* or the *Tn2496* mutant strain, both expressing GFP (green). 7 days post-infection, cells were fixed and labelled with an anti-LAMP1 antibody (red) and Hoechst (blue) to visualize CCVs and host cell nuclei, respectively. Scale bars 10  $\mu$ m. (D) An average of 50000 cells were automatically imaged and analyzed from triplicate experiments for each condition illustrated in C, and the phenotypic profile of the *Tn2496* mutant was compared to that of wt *C. burnetii* and expressed as z-scores over 15 independent features. (E) GFP-expressing *C. burnetii* transformed with plasmids encoding either wt CstK, the K55M or the FFA mutants, all under the regulation of an IPTG-inducible promoters were used to infect U2OS cells for 6 days, in the presence or absence of IPTG. Cells were then fixed and labelled as in C, and an average of 50000 cells were automatically imaged and analyzed for each condition. The mean size of *C. burnetii* colonies and CCVs was calculated (red bars). (F) U2OS cells were challenged either with wt *C. burnetii*, the GFP-expressing mutant *Tn2496* or a combination of the two strains for 6 days. Cells were then fixed and labelled with anti-*C. burnetii* antibodies (anti-NMII) to label both strains. (G) An average of 50000 cells were automatically imaged and analyzed for each condition illustrated in F and the mean size of *C. burnetii* colonies was calculated (red bars). n.s., non-significant; \*\*\*\*,  $p < 0.0001$ , one-way ANOVA, Dunnett's multiple comparison test.

**Figure 4. CstK interacts with TBC1D5.** (A) The interaction between CstK and the human TBC1D5 has been confirmed after cotransfection of HEK-293T cells to express each HA-tagged CstK derivatives with GFP-tagged Hs-TBC1D5. Cells have been lysed and HA-tagged CstK derivatives have been trapped on anti-HA magnetic beads (Pierce). Beads were washed, eluted by boiling, and bound proteins were revealed by Western blot analysis. Anti-HA antibody confirms the immunoprecipitation of CstK derivatives. For the densitometry graph, Regions of Interest (ROIs) were obtained from each band of interest and the intensity was measured (B) Hs\_TBC1D5 localization during infection was monitored in U2OS cells expressing mCherry-tagged Hs-TBC1D5 (red) challenged for 4 days either with wt *C. burnetii*, the *Dot/Icm*-defective *dotA::Tn* mutant or the CstK-overexpressing mutant *Tn2496*, all expressing GFP (green). Lysosomal compartments were labelled with anti-LAMP1 antibodies (blue). Scale bars 10  $\mu$ m. Inset magnification scale bars 4  $\mu$ m (C) The role of TBC1D5 in *C. burnetii* infections was investigated using siRNA to deplete Hs-TBC1D5 in U2OS prior to challenge with GFP-expressing wt *C. burnetii*. The size of CCVs was automatically calculated over an average of 150000 cells per condition. Red bars indicate medians. \*\*\*,  $p < 0.0001$ ; \*\*,  $p < 0.001$ ; \*,  $p < 0.01$ ; one-way ANOVA, Dunnett's multiple comparison test. Scale bars 10  $\mu$ m.

**TABLES**

**Table 1. Strains and plasmids used in this study**

<b>Strains or Plasmids</b>	<b>Genotype or Description <sup>a</sup></b>	<b>Source or Reference</b>
<b><i>Escherichia coli</i> strains</b>		
<i>E. coli</i> TOP10	<i>E. coli</i> derivative ultra-competent cells used to general cloning; F- <i>mcrA</i> D( <i>mrr-hsdRMS-mcrBC</i> ) f80 <i>dlacZ</i> ÄM15 D <i>lacX74 endA1 recA1araD139 D (ara, leu)7697 galU galK rpsL nupG - tonA</i>	Invitrogen
<i>E. coli</i> BL21(DE3)Star	F2 <i>ompT hsdSB(rB2 mB2) gal dcm</i> (DE3); used to express recombinant proteins in <i>E. coli</i>	Stratagene
<b><i>Coxiella burnetii</i> strains</b>		
<i>Coxiella burnetii</i> RSA439 NMII	Wild type (wt) <i>Coxiella burnetii</i> RSA439 NMII non-fluorescent	(55)
<i>Coxiella burnetii</i> Tn2496	<i>Coxiella burnetii</i> RSA439 NMII carrying an Himar1-CAT-GFP cassette 32 bp upstream of CBU_0175, expressing GFP	This study
<i>Coxiella burnetii</i> Tn1832	<i>Coxiella burnetii</i> RSA439 NMII carrying an Himar1-CAT-GFP cassette in the intergenic region between CBU_1847b and CBU_1849, expressing GFP	(43)
<i>Coxiella burnetii</i> Tn292	<i>Coxiella burnetii</i> RSA439 NMII carrying an Himar1-CAT-GFP cassette in CBU_1648 ( <i>dotA</i> ), expressing GFP	(43)
<b>Plasmids</b>		
pGEX(M)	pGEX with a 321-bp <i>EcoRI/BamHI</i> fragment from pET19b introducing a <i>HindIII</i> site in the pGEX polylinker	(56)
pGEX(M) <sub>cstK</sub>	pGEX(M) derivative used to express GST-tagged fusion of CstK (Amp <sup>R</sup> )	This study
pGEX(M) <sub>cstK_K55M</sub>	pGEX(M) derivative used to express GST-tagged fusion of CstK_K55M (Amp <sup>R</sup> )	This study
pGEX(M) <sub>cstK_Y14F</sub>	pGEX(M) derivative used to express GST-tagged fusion of CstK_Y14F (Amp <sup>R</sup> )	This study
pGEX(M) <sub>cstK_Y209F</sub>	pGEX(M) derivative used to express GST-tagged fusion of CstK_Y209F (Amp <sup>R</sup> )	This study

pGEX(M)_ <i>cstK_T232A</i>	pGEX(M) derivative used to express GST-tagged fusion of CstK_T232A (Amp <sup>R</sup> )	This study
pGEX(M)_ <i>cstK_Y14F/Y209F/T232A</i>	pGEX(M) derivative used to express GST-tagged fusion of CstK_Y14F/Y209F/T232A (Amp <sup>R</sup> )	This study
peGFPN1	Vector used for mammalian expression of C-terminal GFP-tagged fusion proteins	Addgene
peGFPN1_Hs-TBC1D5-GFP	peGFP-N1 derivative used to express C-terminal GFP-tagged fusion of Hs_TBC1D5 for mammalian expression	This study
pmCH_Hs-TBC1D5-mCherry	pmCH derivative used to express C-terminal mCherry-tagged fusion of Hs_TBC1D5 for mammalian expression	This study
pRK5_HA_ <i>cstKopt</i>	pRK5_HA derivative used to express N-terminal HA-tagged fusion of CstK codon-optimized for mammalian expression	This study
pRK5_HA_ <i>cstK_K55Mopt</i>	pRK5_HA derivative used to express N-terminal HA-tagged fusion of <i>cstK_K55M</i> codon-optimized for mammalian expression	This study
pRK5_HA_ <i>cstK_FFAopt</i>	pRK5_HA derivative used to express N-terminal HA-tagged fusion of <i>cstK_FFA</i> codon-optimized for mammalian expression	This study
pXDC61K-Blam	Vector with IPTG-inducible expression of Beta-Lactamase (Blam)	(57)
pXDC61K-Blam- <i>cvpB</i>	pXDC61K-Blam derivative used to express Blam-tagged fusion of CvpB	This study
pXDC61K-Blam- <i>cstK</i>	pXDC61K-Blam derivative used to express Blam-tagged fusion of CstK	This study
pJA-LACO-4xHA	Vector with IPTG-inducible expression of 4xHA-tagged proteins	(30)
pJA-LACO-4xHA- <i>cstK</i>	Vector with IPTG-inducible expression of 4xHA-tagged <i>cstK</i>	This study
pJA-LACO-4xHA- <i>cstK_K55M</i>	Vector with IPTG-inducible expression of 4xHA-tagged <i>cstK_K55M</i>	This study
pJA-LACO-4xHA- <i>cstK_FFA</i>	Vector with IPTG-inducible expression of 4xHA-tagged <i>cstK_FFA</i>	This study
<b><i>Dictyostelium discoideum</i> plasmids</b>		
pDXA-3C_ <i>cstK-FLAG</i>	vector for overexpression of CstK with a C-terminal Flag tag in <i>D. discoideum</i>	This study
pDXA-3C_ <i>DdTBC1D5-myc</i>	vector for expression of myc-DdTBC1D5 in <i>D. discoideum</i>	This study

**Table 2. Primers used in this study**

<b>Primers</b>	<b>5' to 3' Sequence<sup>a, b</sup></b>
NtermCstK	TAT <u>GGATCCT</u> TAATGGCTTATATGAGGCTTAGT ( <i>Bam</i> HI)
CtermCstK	TATA <u>AAGCTTT</u> TAATCCCATTCAATATTTTC ( <i>Hind</i> III)
RvCstK K55M	ATAAAAGAGCA <b>T</b> CGCCGCTCG
FwCstKY14F	CTTAGTGTGGCTGACTTTTT <b>T</b> GATTGAAGAAGGGCAAG
FwCstKY209F	GGGGCGACGGGCTATCGCT <b>T</b> CTGTAACCCTCACATAAAG
FwCstKT232A	CATTCGTGAACAGTTTAATGCTGCGGGCCATTTGCGATTAC
CstKopt-BamHI-Fw	GAAGGATCCCTGATGGCGTATATGCGTCTGAG
CstKopt-EcoRI-Rv	CTTGAATTCCTTAGTCCC <b>A</b> CTCGATGTTTTCCAGATG
CstK-KpnI-Fw	AGGGGTACCTTAATGGCTTATATGAGGCTTAGT
CstK-BamHI-Rv	AGGGGATCCTAATTAATCCCATTCAATATTTTCTAA
CvpB-KpnI-Fw	GATGGTACCAGCAGACAGCCATCATTG
CvpB-KpnI-Fw	GATGGTACCAGCAGACAGCCATCATTG

**RT-PCR PRIMERS**

DotA-F	GCTCCCAGCATT <b>C</b> ATCCAGT
DotA-R	GGCACTTAACCAGCCCTCAT
CstK-F	GGCAAGGTATTAGGGCGGAA
CstK-R	GGGATTCTCACCATTGGCCT

<sup>a</sup> Restriction sites are underlined and specified into brackets.

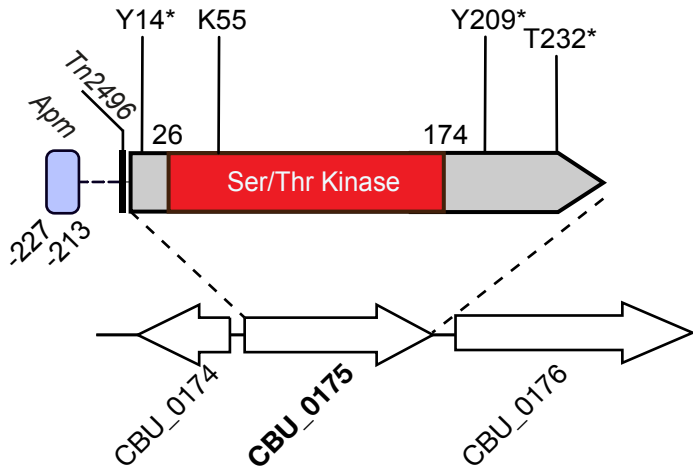
<sup>b</sup> Mutagenized codons are shown in bold.

**Table 3. Phosphoacceptors identified after phosphorylation of *C. burnetii* CstK.** Sequences of the phosphorylated peptides identified in CstK as determined by mass spectrometry following tryptic digestion are indicated, and phosphorylated residues (pT or pY) are shown in bold.

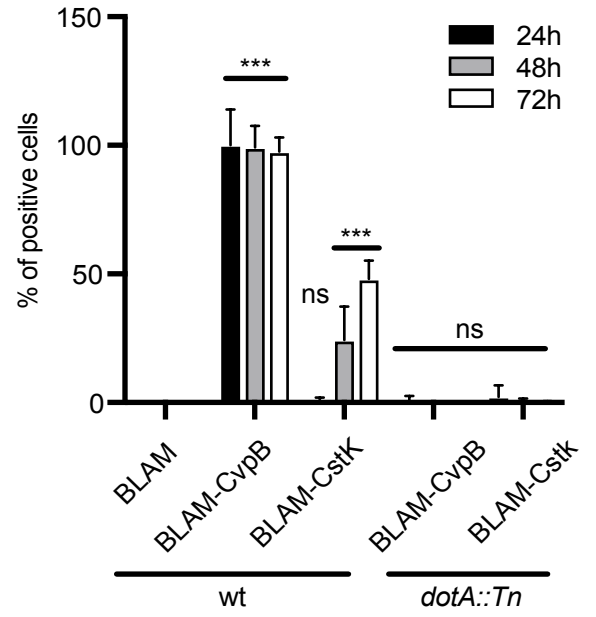
<b>Phosphorylated tryptic peptide sequence of CstK</b>	<b>Number of detected phosphate groups LC/MS/MS</b>	<b>Phosphorylated residue(s)</b>
[8-18] LSVADF <b>p</b> YDLKK	<b>1</b>	<b>Y14</b>
[228-237] EQFN <b>p</b> TAGHLR	<b>1</b>	<b>T232</b>
[209-215] <b>p</b> YCNPHIK	<b>1</b>	<b>Y209</b>

**Figure 1**

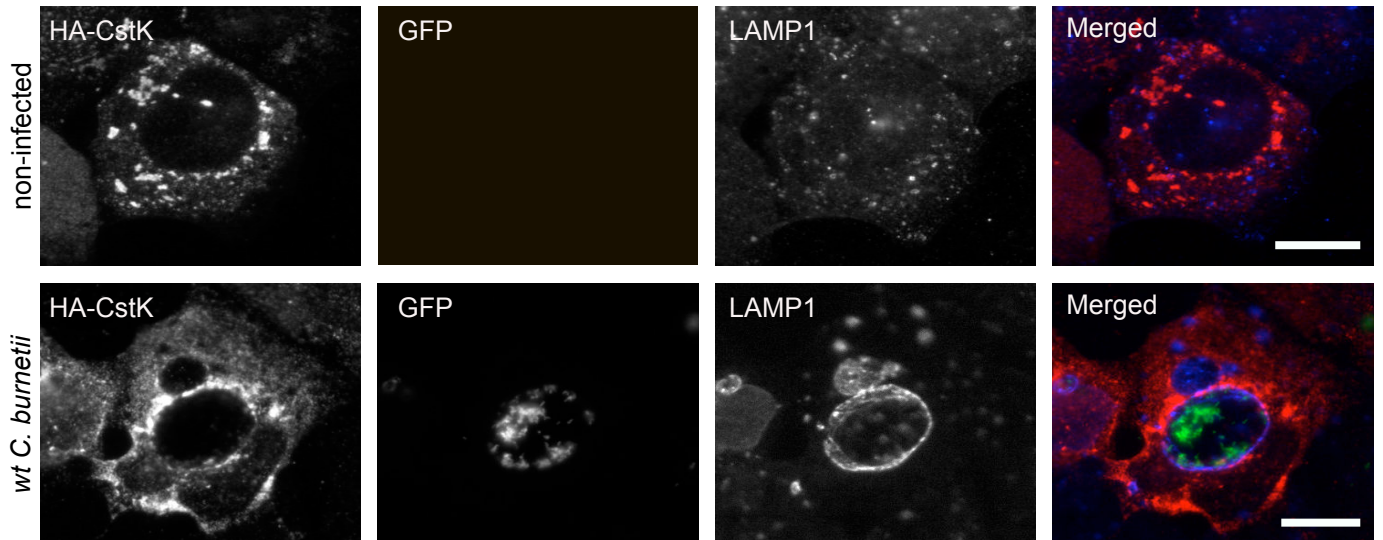
**A**

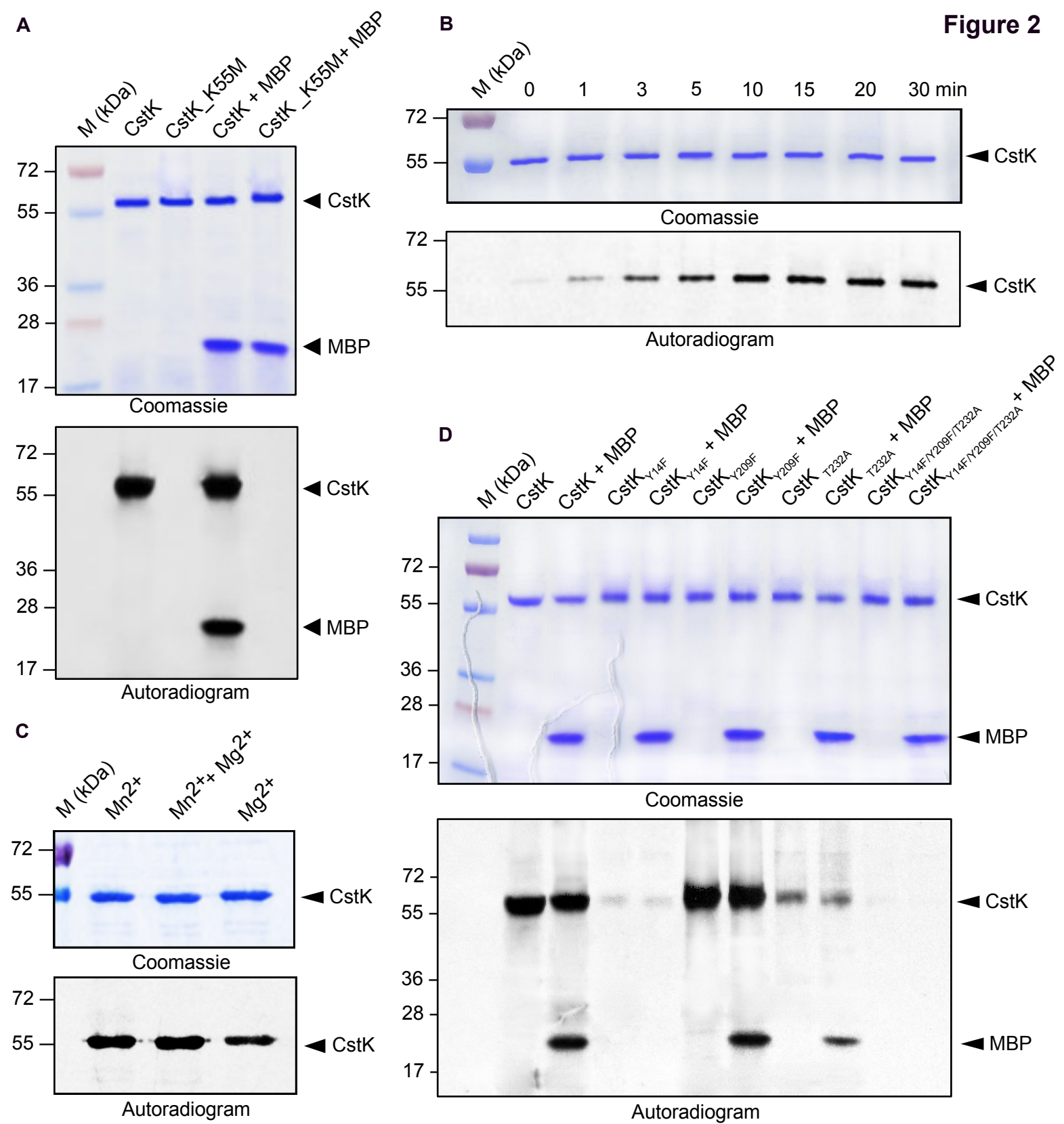


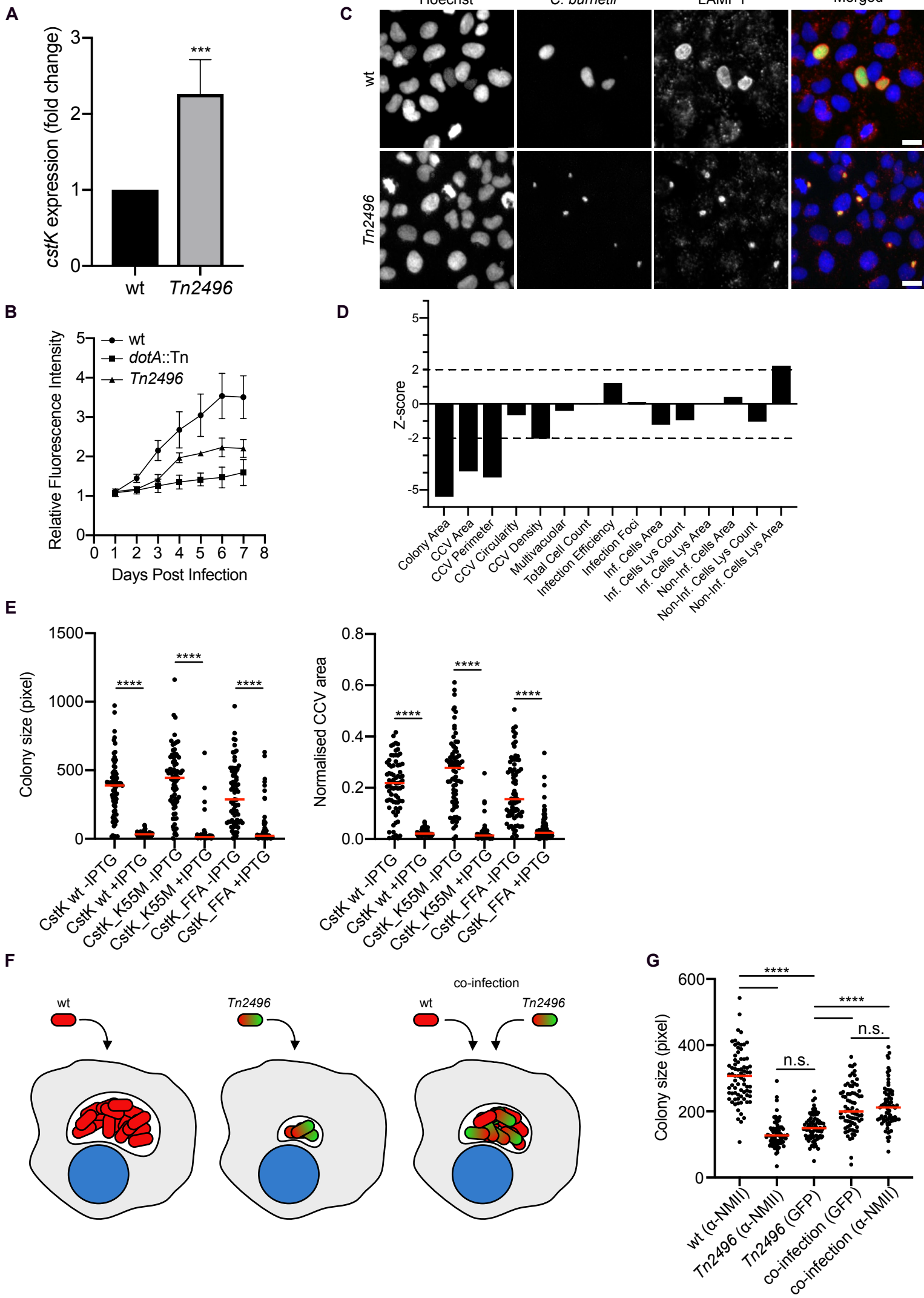
**B**



**C**

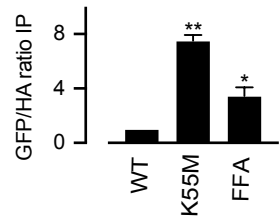
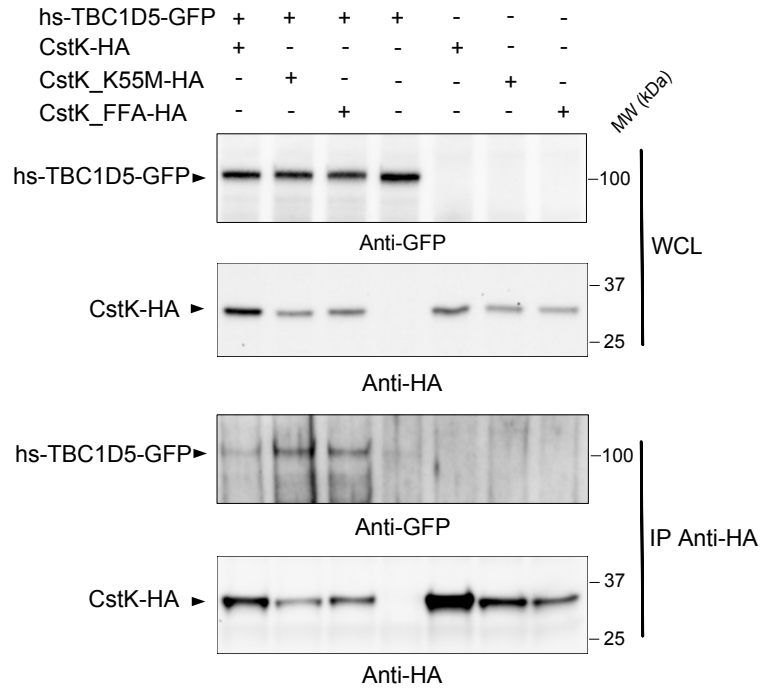




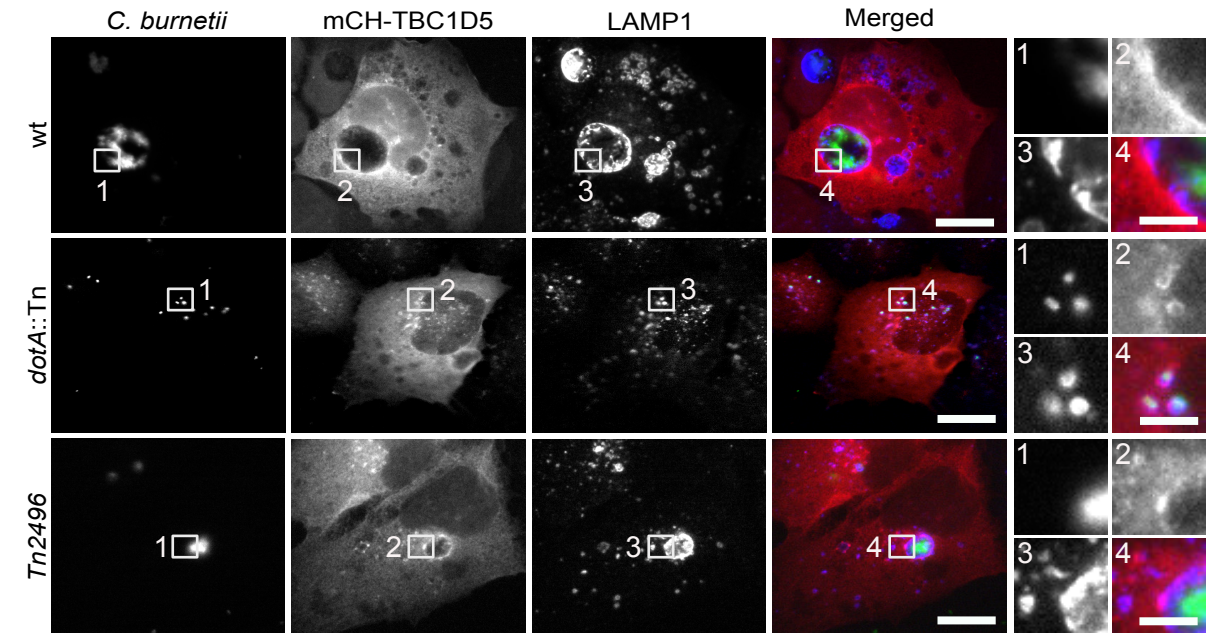
**Figure 3**

**Figure 4**

**A**



**B**



**C**

